FERMILAB-PUB-22-374-T,
MSUHEP-22-017

ResBos2 and the CDF W Mass Measurement

Joshua Isaacson,[1,*] Yao Fu,[2] and C.-P. Yuan[3]

[1] *Theoretical Physics Department, Fermi National Accelerator Laboratory, P.O. Box 500, Batavia, IL 60510, USA*
[2] *Department of Modern Physics, University of Science and Technology of China, Jinzhai Road 96, Hefei, Anhui, 230026, China*
[3] *Department of Physics and Astronomy, Michigan State University, 567 Wilson Road, East Lansing, MI 48824, USA*

The recent CDF W mass measurement of 80,433 ± 9 MeV is the most precise direct measurement. However, this result deviates from the Standard Model predicted mass of 80,359.1 ± 5.2 MeV by 7σ. The CDF experiment used an older version of the ResBos code that was only accurate at NNLL+NLO, while the state-of-the-art ResBos2 code is able to make predictions at N^{3}LL+NNLO accuracy. We determine that the data-driven techniques used by CDF capture most of the higher order corrections, and using higher order corrections would result in a decrease in the value reported by CDF by at most 10 MeV.

In the Standard Model (SM) of particle physics, the electroweak sector can be uniquely determined given 3 input parameters to fix the values of two gauge couplings and the vacuum expectation value, the Higgs and fermion masses, and the weak mixing matrices. One of the predicted results is the mass of the W boson. Currently, the electroweak global fits predict the mass to be 80,359.1 ± 5.2 MeV [1]. Recently, the CDF experiment reported the most precise direct measurement of the W mass as: 80,433 ± 9 MeV [2]. This corresponds to a 7σ deviation from the SM, and has spurred many Beyond the Standard Model explanations [3–55]. However, the ATLAS and LHCb experiments also have directly measured the mass of the W boson and found results of 80,370 ± 19 MeV [56] and 80,354 ± 32 MeV [57], respectively. The tension between the direct measurements are at a level of 3σ, and have raised concerns about the CDF measurement. One major concern brought up is that an older version of the ResBos code [58, 59] was used, which is only at the accuracy of next-to-next-to-leading logarithimic accuracy matched to a next-to-leading fixed order calculation (NNLL+NLO) [60]. Here we investigate the shift in the CDF result that would occur if the state-of-the-art N^{3}LL+NNLO ResBos version 2.0 [61] calculation was used instead, including the correct angular functions at NNLO in Quantum Chromodyamics. We will denote ResBos version 2.0 as ResBos2 for the remainder of the text. Additionally, we consider the effects on the PDF uncertainty from using the higher order prediction.

The ResBos2 calculation includes the cusp anomalous dimension at $\mathcal{O}(\alpha_s^4)$, the non-cusp anomalous dimension at $\mathcal{O}(\alpha_s^3)$, the hard collinear coefficient at $\mathcal{O}(\alpha_s^2)$, and is matched to the fixed order calculation at NNLO. This new accuracy corresponds to an accuracy of N^{3}LL+NNLO as described in Tab. I. The CDF experiment chose to use the same version of ResBos as was used in their previous analysis [62] when the higher order corrections were unknown. The ResBos codebases implement the Collins-Soper-Sterman (CSS) resummation formalism [63, 64], which performs the transverse momentum resummation in b-space as

$$\begin{aligned}\frac{\mathrm{d}\sigma}{\mathrm{d}Q^2\,\mathrm{d}^2\vec{p}_T\,\mathrm{d}y\,\mathrm{d}\cos\theta\,\mathrm{d}\phi} &= \sigma_0 \int \frac{\mathrm{d}^2 b}{(2\pi)^2} e^{i\vec{p}_T\cdot\vec{b}} e^{-S(b)} \\ &\times C\otimes f(x_1,\mu)\, C\otimes f(x_2,\mu) \\ &+ Y(Q,\vec{p}_T,x_1,x_2,\mu_R,\mu_F)\,,\end{aligned} \tag{1}$$

where Q is the invariant mass of the lepton system, $\theta(\phi)$ is the polar (azimuthal) angle in the Collins-Soper frame [65], σ_0 is the leading order matrix element, $x_{1,2} = \frac{Q}{\sqrt{s}} e^{\pm y}$, and Y contains the finite terms of the fixed order calculation in the limit $p_T \to 0$. The Sudakov factor $(S(b))$ is defined as

$$S(b) = \int_{C_1^2/b^2}^{C_2^2 Q^2} \frac{\mathrm{d}\bar{\mu}^2}{\bar{\mu}^2}\left[\ln\left(\frac{C_2^2 Q^2}{\bar{\mu}^2}\right) A\left(\bar{\mu}, C_1\right) + B\left(\bar{\mu}, C_1, C_2\right)\right], \tag{2}$$

and $C\otimes f$ represents the convolution of the hard collinear kernel with the PDF, the values of A, B, and C can be calculated order-by-order in perturbation theory. Additional details and the values of the coefficients needed for N^{3}LL accuracy are given in Appendix A.

Another area of concern is the handling of the angular coefficients within the ResBos code. The angular coefficients are given by

$$\frac{\mathrm{d}\sigma}{\mathrm{d}p_T\,\mathrm{d}y\,\mathrm{d}Q\,\mathrm{d}\cos\theta\,\mathrm{d}\phi} = \frac{3}{16\pi}\frac{\mathrm{d}\sigma}{\mathrm{d}p_T\,\mathrm{d}y\,\mathrm{d}Q}$$

* isaacson@fnal.gov

This manuscript has been authored by Fermi Research Alliance, LLC under Contract No. DE-AC02-07CH11359 with the U.S. Department of Energy, Office of Science, Office of High Energy Physics.

$$\times \Big\{ \left(1+\cos^2\theta\right) + \frac{1}{2}A_0\left(1-3\cos^2\theta\right) + A_1 \sin 2\theta\cos\phi + A_2\sin^2\theta\cos 2\phi \qquad (3)$$
$$+A_3\sin\theta\cos\phi + A_4\cos\theta + A_5\sin^2\theta\sin 2\phi + A_6\sin 2\theta\sin\phi + A_7\sin\theta\sin\phi\Big\}\ .$$

The coefficients A_i are determined order-by-order in the fixed order calculation, with only A_4 being non-zero at leading order. The coefficients $A_{5,6,7}$ are zero until NNLO and are negligible afterwards, and will therefore be ignored in this study. While the matching to NLO was exact in terms of the angular coefficients, it was pointed out that the original matching to NNLO in the RESBOS code did not correctly reproduce the breaking of the Lam-Tung relation [66]. To account for this, the RESBOS2 code uses k-factors obtained from MCFM [67] to correctly reproduce the angular distributions at NNLO accuracy. This effect is expected to be a small effect in the extraction of M_W since the CDF experiment applies a cut of $p_T(W) < 15$ GeV. In the small p_T region all angular coefficients tend towards zero with the exception of the overall leading coefficient and A_4.

To estimate the effects of higher order corrections, we generate pseudoexperiments for the Z and W boson at N^{3}LL+NNLO accuracy with correct angular distributions. The pseudoexperiments use the `CT18NNLO` pdf [68] and fix the non-perturbative function to the BLNY global fit values [59]. These two choices should not have a significant impact on the outcome of the study. The Z boson events are generated satisfying $p_T(Z) < 15$ GeV, $30 < p_T(\ell) < 55$ GeV, $|\eta(\ell)| < 1$, and $66 < M_{\ell\ell} < 116$ GeV. The W boson events are generated satisfying $p_T(W) < 15$ GeV, $30 < p_T(\ell) < 55$ GeV, $30 < p_T(\nu) < 55$ GeV, $|\eta(\ell)| < 1$, and $60 < m_T < 100$ GeV. Here, m_T is the transverse mass and is defined as

$$m_T^2 = 2\left(p_T(\ell)p_T(\nu) - \vec{p}_T(\ell)\cdot\vec{p}_T(\nu)\right), \qquad (4)$$

where $\vec{p}_T(\ell,\nu)$ is the vector transverse momentum and the dot product is related to the difference in ϕ angle between the two vectors. These selection criteria are consistent with those used by CDF. After the selection criteria, CDF had a selection of 1,811,700 (66,180) $W\to e\nu$ ($Z\to ee$) events and 2,424,486 (238,534) $W\to\mu\nu$ ($Z\to\mu\mu$) events [2]. When displaying the statistical uncertainty from CDF in figures, we will use the electron numbers since the background and effects from final state radiation (FSR) are significantly smaller. The main difference is the cut on the $p_T(Z)$, which was chosen to be 15 GeV vs. 30 GeV. This choice should not have an impact on the final extracted mass, and was made to appropriately tune the prediction with the information provided by CDF. The width of the W boson was fixed to 2.0895 GeV to be consistent with the value used by CDF [2], the impact of the width has a minor effect on the extraction of the mass (see App. D), and thus fixing the value does not impact the conclusions of this work.

The CDF experiment used data driven techniques to tune the RESBOS prediction to reproduce the $p_T(Z)$ data. The tuning of the RESBOS prediction involved modifying the values of the g_2 parameter in the BLNY functional form and adjusting the value of $\alpha_s(M_Z)$ used. To mimic the procedure carried out by CDF, we fit the value of g_2 and $\alpha_s(M_Z)$ in the NNLL+NLO prediction to reproduce the transverse momentum spectrum of the Z boson at N^{3}LL+NNLO, and validate it against the W boson transverse momentum. We find that the best fit result comes from using $g_2 = 0.662$ GeV^2 and $\alpha_s(M_Z) = 0.120$, as shown in Fig. 1. To correctly account for the modified value of $\alpha_s(M_Z)$, we used the `CT18NNLO_as_0120` PDF set for the RESBOS prediction at NNLL+NLO.

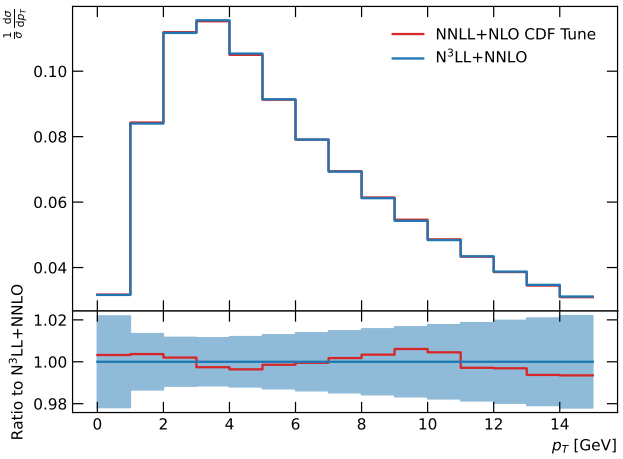

FIG. 1. Comparison of the generated pseudodata for the Z transverse momentum for the state-of-the-art RESBOS2 calculation at N^{3}LL+NNLO (blue) accuracy compared to the NNLL+NLO (red) prediction tuned to the Z transverse momentum distribution. The blue band represents the statistical uncertainty of the CDF result.

Another major concern related to the prediction of the $p_T(Z)$ and $p_T(W)$ distribution is in the effect higher order corrections have on their ratio. We investigate the shift in this ratio in Fig. 3. We take the more aggressive estimate of the uncertainty using correlated scale variations. Even with this aggressive estimate, we find that the ratio is not very sensitive to higher order corrections. Therefore, we expect the impact of using the state-of-the-art RESBOS2 prediction for this ratio will only result in a negligible effect on the extracted W mass. The CDF experiment [2] used DYQT [69, 70] to estimate the uncertainty induced by this ratio, and we leave the validation of this systematic uncertainty to a future work.

The tuned prediction is then used to produce a series of templates to be used to extract the W boson mass in m_T,

Order	Boundary Condition (C)	Anomalous Dimension γ_i (B)	Anomalous Dimension Γ_{cusp} (A)	Fixed Order Matching (Y)
LL	1	-	1-loop	-
NLL	1	1-loop	2-loop	-
NLL' (+ NLO)	α_s	1-loop	2-loop	α_s
NNLL (+ NLO)	α_s	2-loop	3-loop	α_s
NNLL' (+ NNLO)	α_s^2	2-loop	3-loop	α_s^2
N^{3}LL (+ NNLO)	α_s^2	3-loop	4-loop	α_s^2
N^{3}LL' (+ N^{3}LO)	α_s^3	3-loop	4-loop	α_s^3
N^{4}LL (+ N^{3}LO)	α_s^3	4-loop	5-loop	α_s^3

TABLE I. The definitions for the accuracy of the resummation calculation. The accuracy used by CDF was NNLL + NLO, while the state-of-the-art is N^{3}LL + NNLO.

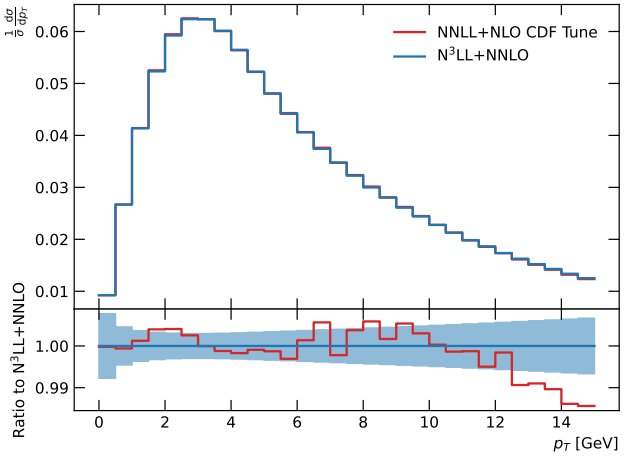

FIG. 2. Comparison of the generated pseudodata for the W transverse momentum for the state-of-the-art ResBos2 calculation at N^{3}LL+NNLO (blue) accuracy compared to the NNLL+NLO (red) prediction tuned to the Z transverse momentum distribution. The blue band represents the statistical uncertainty of the CDF result.

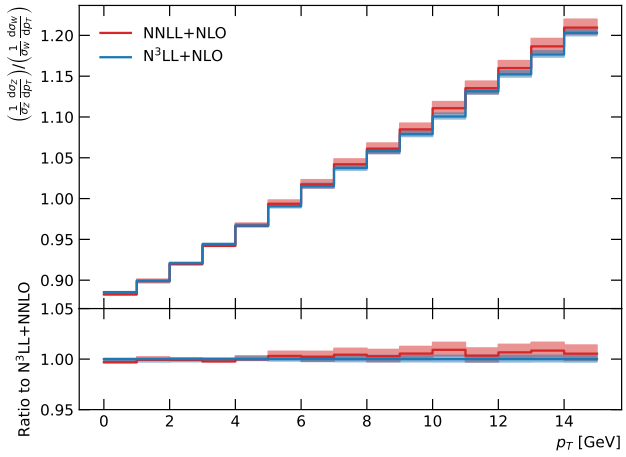

FIG. 3. The ratio for the normalized Z transverse momentum to the normalized W transverse momentum in the region used by the CDF experiment. The NNLL+NLO (red) prediction and the N^{3}LL+NNLO (blue) prediction are consistent with each other over this region. The scale uncertainty is treated in a fully correlated manner.

$p_T(\ell)$, and $p_T(\nu)$, this is based on the procedure used by CDF [2]. We find that the higher order corrections can induce a shift in the W boson mass of less than 10 MeV, with the result being consistent with zero within the statistical accuracy of CDF. The results are given for each observable in Tab. II. The shift without detector and final state QED radiation (FSR) effects is largest for the $p_T(\nu)$ distribution with a shift of 6.6 MeV, while including detector effects reduces the shift for all observables but m_T. Details on the detector smearing effects can be found in Appendix C. The comparison of the tuned result to the pseudoexperiment is shown in Figs. 4, 5, and 6. Thus, we conclude that the tuning of the NNLL+NLO prediction to reproduce the CDF Z transverse momentum data helps to capture the most important higher order corrections. We also conclude that redoing the analysis will not resolve the tension between CDF and the SM, and at most would amount in a decrease in the CDF value by 10 MeV.

Finally, concerns pertaining to the PDF uncertainty quoted by CDF were raised as being too small. CDF claims an uncertainty from the PDFs of 3.9 MeV [2] from the `NNPDF3.1 NNLO` set [71]. With a shift in the central value of ± 2 MeV [2] from considering `CT18` [68] and `MMHT2014` [72] at NNLO. Additionally, CDF looked at the impact from the NLO sets for `ABMP16` [73], `CJ15` [74], `MMHT2014` [72], `NNPDF3.1` [71], and `CT18` [68]. Here they found a shift of ± 3 MeV neglecting `CT18`, and ± 6 MeV including `CT18`. The ResBos prediction used by CDF used the `CTEQ6M` PDF [75], and they found the mass shift from `CTEQ6M` to `NNPDF3.1 NNLO` was $+(3.3, 3.6, 3.0)$ MeV for the (m_T, p_T^ℓ, p_T^ν) fits, respectively [2]. We repeated the study of the PDF uncertainties at N^{3}LL+NNLO for `NNPDF3.1`, `MMHT2014`, and `CT18` at NNLO and NLO, and `CTEQ6M` at NLO using the technique described in Ref. [76]. We find that the PDF uncertainty from `CT18NNLO` is (1.3, 15.9, 15.5) MeV without including detector effects for (m_T, $p_T(\ell)$, and $p_T(\nu)$). In the CDF fit, the total combination is dominated by the m_T result ($\sim 65\%$), with the charged lepton p_T channel accounting for $\sim 25.4\%$ [2]. Since it is unclear how to appropriately propagate the un-

	Mass Shift [MeV]	
Observable	ResBos2	+Detector Effect+FSR
m_T	1.5 ± 0.5	$0.2 \pm 1.8 \pm 1.0$
$p_T(\ell)$	3.1 ± 2.1	$4.3 \pm 2.7 \pm 1.3$
$p_T(\nu)$	4.5 ± 2.1	$3.0 \pm 3.4 \pm 2.2$

TABLE II. Summary of the shift in M_W due to higher order corrections. For reference, the CDF result was 80,433 ± 9 MeV [2] and the SM predicted value is 80,359.1 ± 5.2 MeV [1]. The second column shows the shift in the mass neglecting detector effects and final state radiation (FSR), while the third column includes an estimate for detector effects and FSR in the mass shift. The first uncertainty is the statistical uncertainty induced in the mass extraction due to the number of ResBos events generated for the pseudoexperiments and the mass templates. The second uncertainty is the detector effect uncertainty calculated by using 100 different smearings of the data to extract the W mass. Additional details on the smearing can be found in Appendix C.

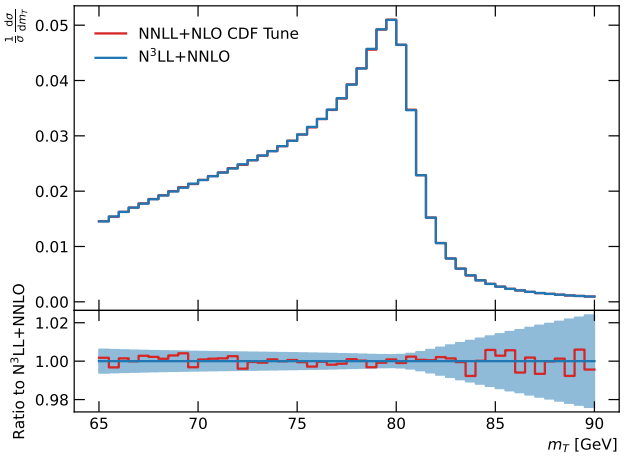

FIG. 4. W mass fit results to the pseudoexperiment for m_T. The pseudodata is generated at N^{3}LL+NNLO accuracy with the default BLNY parametrization. The tuned NNLL+NLO results are then used for a template fit to extract the W mass [2]. The tuning resulted in a best fit value of $g_2 = 0.66$ GeV^{-2} and $\alpha_s(M_Z) = 0.120$. The best fit mass (80,386 MeV) is shown in red. The blue band represents the statistical uncertainty of the CDF result. Detector effects and FSR are not included here, but the corresponding result for m_T can be found in Appendix C.

certainties from individual observables to the final mass extraction, we just quote the results from the dominant m_T observable. The shifts found in the W mass using m_T for the various PDFs are shown in Tab. III, with additional details for the other observables in Appendix E. The PDF uncertainties that we find are consistent with the 3.9 MeV quoted by CDF [2].

In conclusion, two of the major criticisms leveled against the theory calculations involved in the ResBos program cannot explain the deviation from the SM that is reported by CDF. We found that the data-driven techniques used by the CDF experiment help to reduce the

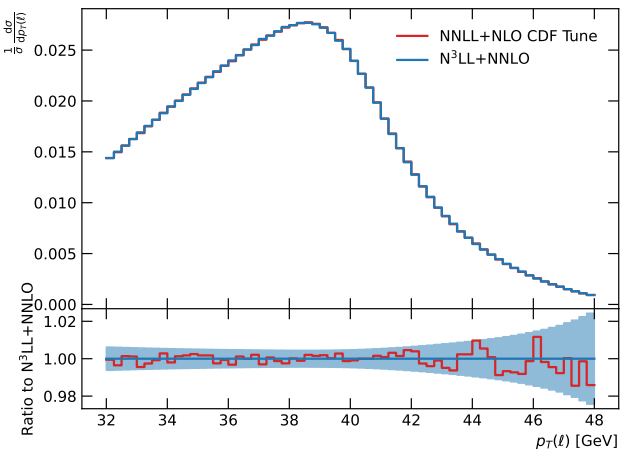

FIG. 5. Similar to Fig. 4 but using $p_T(\ell)$ to extract the W mass. The best fit mass (red) is 80,388 MeV.

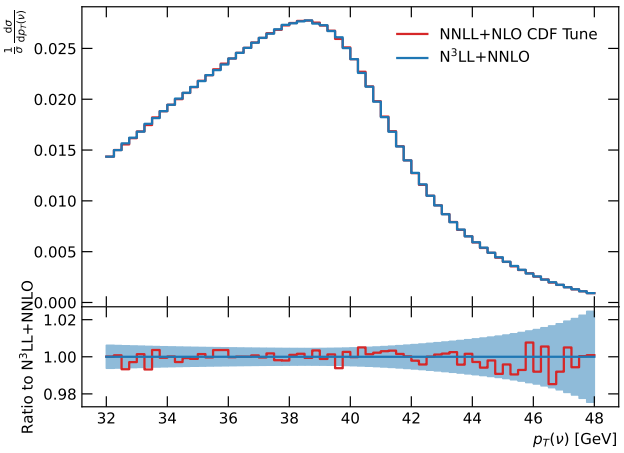

FIG. 6. Similar to Fig. 4 but using $p_T(\nu)$ to extract the W mass. The best fit mass (red) is 80,389 MeV.

effects of higher order corrections. The estimated shift due to including these corrections is at most 10 MeV, and may reduce the disagreement from 7σ to 6σ. The PDF uncertainty is found to be consistent with the numbers quoted by CDF. While there remain main questions pertaining to the CDF result, we have addressed the most important questions related to the theory calculations

	m_T	
PDF Set	NNLO	NLO
`CT18`	0.0 ± 1.3	1.8 ± 1.2
`MMHT2014`	1.0 ± 0.6	2.6 ± 0.6
`NNPDF3.1`	1.1 ± 0.3	2.1 ± 0.4
`CTEQ6M`	N/A	2.8 ± 0.9

TABLE III. Comparison of the shift of M_W for different PDF sets using the m_T observable. The central prediction used was `CT18NNLO` with a mass of 80,385 MeV. The uncertainties quoted are the PDF uncertainties for the given PDF set.

used, and have found no major mass shift.

ACKNOWLEDGMENTS

We thank John Cambell for help with the MCFM code. We thank Simone Amoroso, Joshua Bendavid, Maarten Boonekamp, Tao Han, Joey Huston, Ashutosh Kotwal, Pavel Nadolsky, Boris Tuchming, Mika Anton Vesterinen, Michael Wagman, and Feng Yuan for helpful discussions. We thank Stefan Höche and Pedro Machado for comments on the manuscript. This manuscript has been authored by Fermi Research Alliance, LLC under Contract No. DE-AC02-07CH11359 with the U.S. Department of Energy, Office of Science, Office of High Energy Physics. It is also supported in part by the U.S. National Science Foundation under Grant No. PHY-2013791. C.-P. Yuan is also grateful for the support from the Wu-Ki Tung endowed chair in particle physics.

Appendix A: Collins-Soper-Sterman Formalism

There are many different formalisms used to perform the resummation of the transverse momentum of color singlet final states, including the CSS formalism [64, 65], the CFG formalism [77], resummation in direct p_T space [78], SCET formalisms [79–81], and TMD formalisms [82, 83]. The ResBos2 code implements both the CSS and CFG formalism (both of which are closely related to the TMD formalism). The version of the ResBos code used by the CDF collaboration only implements the CSS formalism, the shift in the W mass induced by different formalisms is an ongoing work.

The CSS formalism was introduced in Ref. [65], and uses impact parameter space to formally resum the logarithmic terms in the fixed order calculation. This involves solving the renormalization group equations (RGE) given by

$$\frac{d}{d\log\mu}K\left(b\mu, g_s\left(\mu\right)\right) = -\gamma_K\left(g_s\left(\mu\right)\right)K\left(b\mu, g_s\left(\mu\right)\right), \tag{A1}$$

$$\frac{d}{d\log\mu}G\left(b/\mu, g_s\left(\mu\right)\right) = \gamma_K\left(g_s\left(\mu\right)\right)G\left(b/\mu, g_s\left(\mu\right)\right), \tag{A2}$$

where γ_K is the anomalous dimension given by

$$\gamma_K = \Gamma_{\text{cusp}}\log(Q^2/\mu^2) + \gamma_i \tag{A3}$$

The logarithms that are resummed are determined by the order of the cusp (Γ_{cusp}) and non-cusp (γ_i) annomalous dimensions. These result in the order of the A and B coefficients in the CSS formalism (see Eq.(2)). The values for $A^{(1)}$, $A^{(2)}$, $A^{(3)}$, $B^{(1)}$ and $B^{(2)}$ are given as

$$A^{(1)} = C_F, \tag{A4}$$

$$A^{(2)} = \frac{1}{2}C_F\left(\left(\frac{67}{18} - \frac{\pi^2}{6}\right)C_A - \frac{5}{9}N_f\right), \tag{A5}$$

$$\begin{aligned} A^{(3)} = C_F\Bigg(&\frac{C_F N_f}{2}\left(\zeta_3 - \frac{55}{48}\right) - \frac{N_f^2}{108} \\ &+C_A^2\left(\frac{11\zeta_3}{24} + \frac{11\pi^4}{720} - \frac{67\pi^2}{216} + \frac{245}{96}\right) \\ &+C_A N_f\left(\frac{-7\zeta_3}{12} + \frac{5\pi^2}{108} - \frac{209}{432}\right)\Bigg), \end{aligned} \tag{A6}$$

$$B^{(1)} = -\frac{3}{2}C_F, \tag{A7}$$

$$\begin{aligned} B^{(2)} = &C_F^2\left(\frac{\pi^2}{4} - \frac{3}{16} - 3\zeta_3\right) \\ &+ C_F C_A\left(\frac{11}{36}\pi^2 - \frac{193}{48} + \frac{3}{2}\zeta_3\right) \\ &+ C_F N_f\left(\frac{17}{24} - \frac{\pi^2}{18}\right), \end{aligned} \tag{A8}$$

where $C_F = 4/3$, $C_A = 3$, and N_f is the number of active quarks used in the running of the β function. The values for $A^{(4)}$ are given in Refs. [84, 85], and for $B^{(3)}$ in Ref. [86]. The hard collinear coefficient at $\mathcal{O}(\alpha_s)$ is given as

$$C_{qq}^{(1)}(z) = \frac{1}{2}C_F(1-z) + \delta(1-z)\frac{1}{4}C_F\left(\pi^2 - 8\right), \tag{A9}$$

$$C_{qg}^{(1)}(z) = \frac{1}{2}z(1-z), \tag{A10}$$

$$C_{q\bar{q}}^{(1)}(z) = C_{qq'}^{(1)}(z) = C_{q\bar{q}'}^{(1)}(z) = 0, \tag{A11}$$

and the coefficient at $\mathcal{O}(\alpha_s^2)$ are given in Ref. [87].

1. Non-Perturbative Function

In the resummation calculation, the lower limit of the integral in Eq. (2) results in evaluating the strong coupling constant at a scale in which it becomes non-perturbative. To handle this issue, a prescription needs to be introduced to ensure the perturbative calculation remains perturbative. In this work, we use the b^* prescription [65]

$$b^* = \frac{b}{\sqrt{1 + \frac{b^2}{b_{\text{max}}^2}}}, \tag{A12}$$

where b_{max} is a parameter fixed to determine the maximum allowed b value. To be consistent with the calculation used by CDF, we choose to take $b_{\text{max}} = 0.5\ \text{GeV}^{-1}$. This converts Eq. (2) into two contributions

$$S(b) = S_{\text{NP}}S_{\text{Pert}}, \tag{A13}$$

$$\begin{aligned} S_{\text{Pert}}(b) = \int_{C_1^2/(b^*)^2}^{C_2^2Q^2}\frac{\mathrm{d}\bar{\mu}^2}{\bar{\mu}^2}\Bigg[&\ln\left(\frac{C_2^2Q^2}{\bar{\mu}^2}\right)A\left(\bar{\mu}, C_1\right) \\ &+B\left(\bar{\mu}, C_1, C_2\right)\Bigg]. \end{aligned}$$

The functional form of S_{NP} is fit to data, and the parametrization used is inspired by the evolution of the Collins-Soper kernel.

CDF used the Brock-Landry-Nadolsky-Yuan (BLNY) non-perturbative functional form fit to global data within their analysis [59, 88]. The functional form is given as:

$$S_{\rm NP} = \left[-g_1 - g_2 \ln\left(\frac{Q}{2Q_0}\right) - g_1 g_3 \ln\left(100 x_1 x_2\right)\right] b^2 \,, \tag{A14}$$

where Q_0 is fixed to 1.6 GeV. The parameters g_1, g_2, and g_3 are constrained from the combined fit to the low transverse momentum distributions of Drell-Yan lepton pair production with 4 GeV $< Q <$ 12 GeV in fixed target experiments and W and Z production ($Q \sim 90$ GeV) at the Tevatron. The best fit gives the values: $g_1 = 0.21$, $g_2 = 0.68$, and $g_3 = -0.60$ [59, 88].

An investigation into the impact of flavor dependence of the non-perturbative function and the choice of functional form on the extracted W mass is left to a future work. Some preliminary estimates for the flavor dependence effects for the ATLAS measurement were studied in Ref. [89]. Additionally, lattice QCD calculations of TMDs, the non-perturbative function, and flavor dependence are an active area of research [90–100]. Detailed studies on the impact of these results on the extraction of the W mass are needed.

Appendix B: Angular Coefficients

As previously discussed, the ResBos2 code uses MCFM [67] to correct the angular coefficients to be accurate at NNLO. The impact of these coefficients at the Tevatron on the W mass extraction are expected to be small. The most important distribution to consider when measuring the W mass at the Tevatron is the difference in azimuthal angle between the lepton and the missing momentum in the lab frame used in calculating m_T ($\Delta\phi$), see Eq. (4). Figure 7 shows the comparison between the result for N^{3}LL+NNLO accuracy compared to NNLL+NLO accuracy. The uncertainty is the statistical uncertainty quoted by CDF. We find that this distribution is stable to the order of the calculation, and thus changing the order would not have a noticeable impact on the W mass measurement. A comparison of the angular coefficients to the results from the LHC is left to a future work.

Appendix C: Detector Smearing and Final State Radiation Effects

The ResBos code does not contain final state QED radiation (FSR) nor detector effects in the calculation. These effects smear out the observables used to measure the W mass, especially m_T. To investigate the impact of these effects, we parameterize the smearing effect and

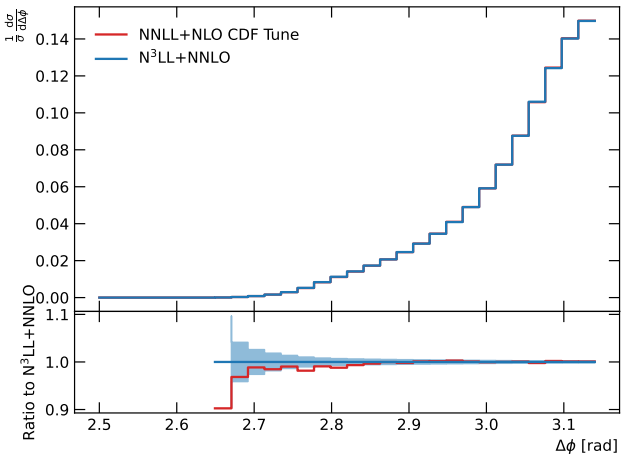

FIG. 7. Comparison of the generated pseudodata for $\Delta\phi$ using the N^{3}LL+NNLO calculation compared to the CDF tuned prediction at NNLL+NLO. The blue band represents the statistical uncertainty associated with the CDF measurement.

fit it to the data observed by CDF. In particular, we chose to study the electron channel since the impact of FSR and the background are both smaller than the muon channel. The comparison of the tuned smearing to the CDF data can be seen in Fig. 8. We used a three parameter fit to determine the width of the Gaussian based on the energy of the particle given by $\frac{\sigma}{E} = a \oplus \frac{b}{\sqrt{E}} \oplus \frac{c}{E}$, where a, b, and c are the parameters of the fit, and the terms are added in quadrature to obtain the width. Both the pseudodata and the mass templates are smeared using the same functional form, and the results are given in Tab. II. This form will not capture the detection efficiency nor all of the FSR effects, but can reproduce the general shape of the m_T distribution shown in Fig. 8. We leave a detailed study of FSR to a future work, and require additional information from the CDF collaboration to accurately model the detector acceptance.

To estimate the impact of the approximation of the detector response on the extraction of M_W, we preform an additional check in which a simple Gaussian with a width of 5% for electrons and 11% for neutrinos is used to smear the results. The comparison between the two approaches are given in Tab. IV. We find that the choice of smearing does not have an impact on the extracted result of M_W, so long as the smearing of the data and the templates are identical. The accuracy of the model used by CDF to smear the theory templates is beyond the scope of this work, but the inaccuracy of our model compared to that used by CDF does not change the conclusions drawn within this work.

Appendix D: Width Effects

In the extraction of the W mass, the CDF experiment kept fixed the width of the W boson to 2.0895 GeV. We

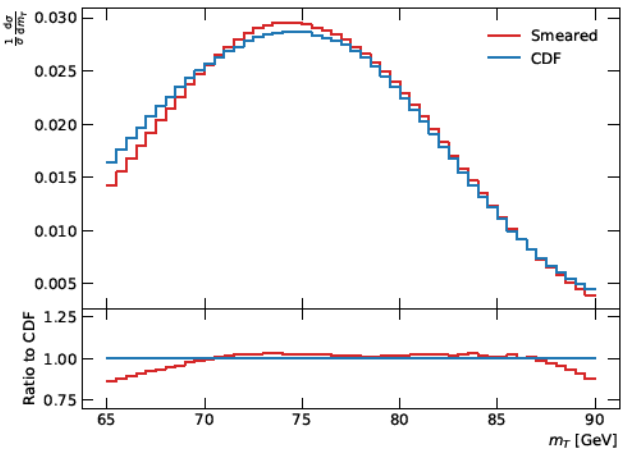

FIG. 8. Comparison of the smeared m_T distribution to the CDF data. The red curve is the result of the smearing, and the blue curve is the extracted CDF data in the electron channel.

	Mass Shift [MeV]	
Observable	Smearing 1	Smearing 2
m_T	$0.2 \pm 1.8 \pm 1.0$	$1.0 \pm 2.1 \pm 1.3$
$p_T(\ell)$	$4.3 \pm 2.7 \pm 1.3$	$4.5 \pm 2.6 \pm 1.4$
$p_T(\nu)$	$3.0 \pm 3.4 \pm 2.2$	$3.8 \pm 4 \pm 2.7$

TABLE IV. Summary of the shift in M_W due to two different smearing methods. The first uncertainty denotes the statistical uncertainty, and the second uncertainty results from an approximate model simulating the detector effect and FSR, calculated from generating 100 different smearings on the data. "Smearing 1" refers to the fit result to the CDF data, and "Smearing 2" refers to the crude Gaussian smearing.

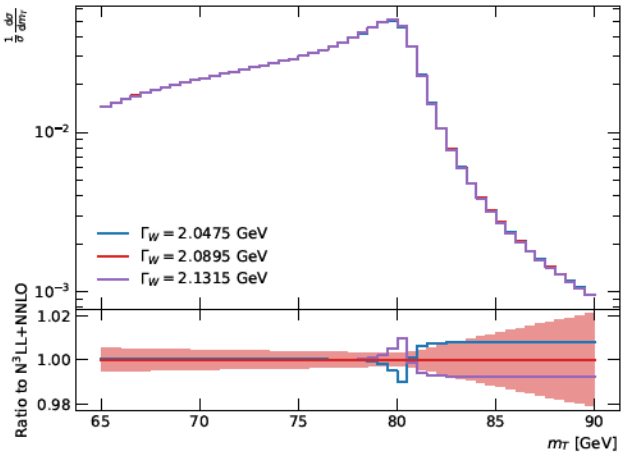

FIG. 9. Comparison of the m_T distribution for various different choices of Γ_W. The width used by CDF was 2.0895 GeV (red curve), and the blue and purple curve represent the shift in the width up and down by one standard deviation of the uncertainty quoted by the PDG [101].

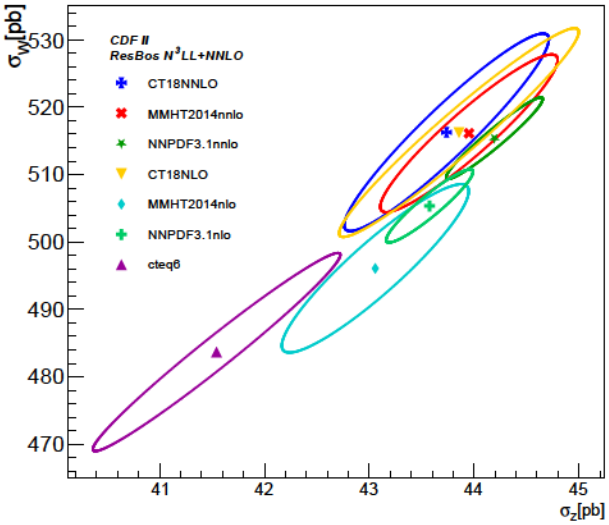

FIG. 10. PDF-induced correlation ellipses, at the 68% confidence level (C.L.), between the fiducial cross sections of W and Z boson production at the Tevatron Run II.

follow the approach taken by CDF and write the propagator of the W boson as a Breit-Wigner shape with an energy-dependent width. The couplings of gauge bosons to fermions are defined in the G_μ scheme. To estimate the impact of varying the width on the CDF result, we varied the width by 0.042 GeV based on the uncertainty from the global width measurement from the PDG [101]. Additionally, a fourth variation was used in which the width was fixed to the Standard Model prediction for the width at NLO, in which the width is proportional to M_W^3. The experimental observable most sensitive to the width is m_T, and thus we only preformed the extraction for this observable. The effect of the width on m_T can be found in Fig. 9, where the red uncertainty band gives the statistical uncertainty from CDF. It is clear that the effect of the width is important at high m_T (*i.e.* $m_T > 80$ GeV). Table V shows the extracted mass shift for the different mass scenarios described above.

Width	Mass Shift [MeV]
2.0475 GeV	2.0 ± 0.5
2.1315 GeV	0.3 ± 0.5
NLO	1.2 ± 0.5

TABLE V. The shift in M_W due to changing the width. The width is varied by the uncertainty from the PDG [101], with the central value set to 2.0895 GeV used by the CDF collaboration [2]. Additionally, the Standard Model prediction for the width at NLO is considered.

Appendix E: PDF-induced Correlations

In Table III, we compared the shift of M_W for different PDF sets using the m_T observable. Similar comparisons

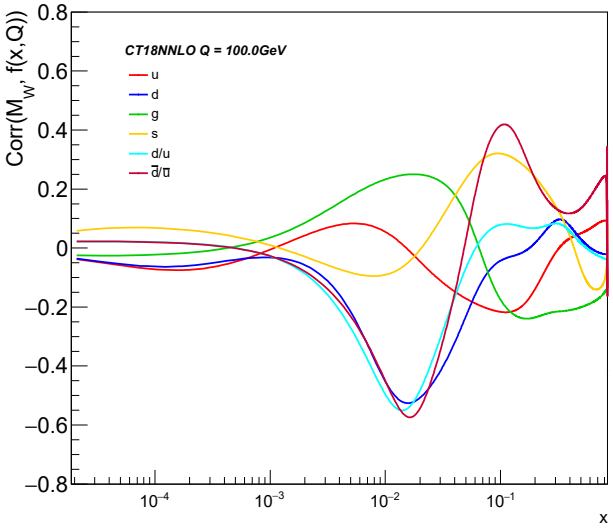

FIG. 11. PDF-induced correlation cosine between the extracted W boson mass (from m_T distribution) and the CT18 NNLO PDFs at the specified x value with $Q = 100$ GeV.

using the $p_T(\ell)$ and $p_T(\nu)$ observables are listed in Table VI. Again, the central prediction used was `CT18NNLO` with a mass of 80,385 MeV. The uncertainties quoted are the PDF uncertainties for the given PDF set. As noted in the main text, it is unclear to us how to appropriately propagate the uncertainties from individual observables to the final mass extraction done by CDF.

Below, we briefly summarize a few PDF-induced correlations, predicted at N^{3}LL+NNLO, relevant to the CDF analysis.

Fig. 10 shows the PDF-induced correlation ellipses between the fiducial cross sections of W and Z boson productions (σ_W vs. σ_Z) at the Tevatron Run II for various PDF sets. Here, the kinematic cuts, as discussed in the main text, have been imposed. Fig. 11 displays the PDF-induced correlation of M_W (extracted from the m_T distribution) and CT18 NNLO error PDFs, for various flavors as a function of x at $Q = 100$ GeV. It shows that at the typical value of x, for the inclusive production of W boson at the Tevatron, around $M_W/\sqrt{S} \simeq 80/1960 \simeq 0.04$, the PDF-induced error in M_W is mainly correlated to that of the PDF-ratios $\bar{d}/\bar{u}$, d/u and d-PDFs. As discussed in Refs. [102, 103], one can easily find the first few leading eigenvector (EV) sets of error PDFs relevant to a particular experimental observable, such as the m_T distribution, by applying the ePump-optimization procedure. This application of ePump (error PDF Updating Method Package) is based on ideas similar to that used in the data set diagonalization method developed by Pumplin [104]. It takes a set of Hessian error PDFs and constructs an equivalent set of error PDFs that exactly reproduces the Hessian symmetric PDF uncertainties, but in addition

each new eigenvector pair has an eigenvalue that quantitatively describes its contribution to the PDF uncer-

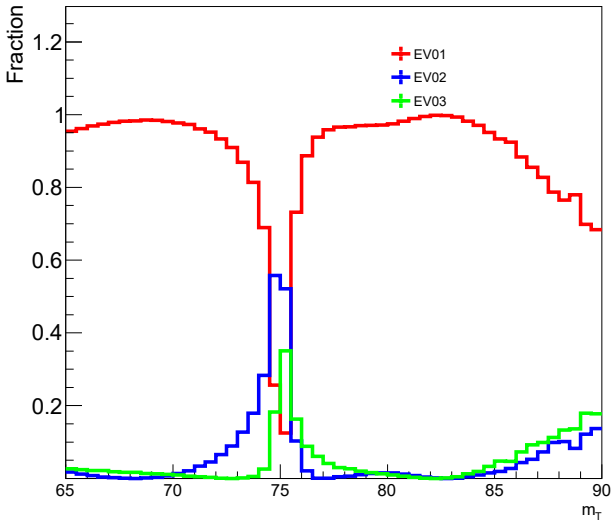

FIG. 12. Fractional contribution of the three leading optimized eigenvector PDFs (EV01, EV02 and EV03) to the variance of the m_T distribution, normalized to each bin, obtained from the ePump-optimization analysis.

can be considered as projecting the original error PDFs to the given data set, and be optimized or re-ordered so that it is easy to choose a reduced set that covers the PDF uncertainty for the input data set to any desired accuracy [102, 103]. The result is shown in Figs. 12 and 13. The eigenvalues of the three leading EV sets, after applying the ePump-optimization, are 44.5, 3.0, 2.4, respectively. The combination of those top three optimized error PDFs contributes up to 99.6% in the total PDF variance of the 50 given data points, *i.e.,* with 50 bins in m_T distribution. This ePump-optimization allows us to conveniently use these three leading new eigenvectors (with a total of six error sets), in contrast to applying the full 58 error sets of the CT18 NNLO PDFs, to study the PDF-induced uncertainty of the m_T observable. Among them, the leading set EV01 dominates the Jacobian region, for m_T around M_W. Hence, one could use those three leading pairs of EV sets to perform Monte Carlo study, such as studying the detector effect on the determination of M_W. The contributions provided by those three pairs of eigenvector PDFs to the PDF-induced uncertainty of m_T distribution, for various parton flavors and x-ranges, are depicted in Fig. 13. The first eigenvector pair (EV01) gives the largest PDF contribution to the m_T uncertainty, dominates the d and $\bar{d}/\bar{u}$ uncertainties in the x region of the W boson production at the Tevatron. In the same figure, we also show the other two noticeable contributions of those three leading EV sets, which are found in the strangeness and gluon PDFs.

	m_T		$p_T(\ell)$		$p_T(\nu)$	
PDF Set	NNLO	NLO	NNLO	NLO	NNLO	NLO
`CT18`	0.0 ± 1.3	1.8 ± 1.2	0.0 ± 15.9	2.0 ± 14.3	0.0 ± 15.5	2.9 ± 14.2
`MMHT2014`	1.0 ± 0.6	2.6 ± 0.6	6.2 ± 7.8	36.7 ± 7.0	3.9 ± 7.5	36.0 ± 6.7
`NNPDF3.1`	1.1 ± 0.3	2.1 ± 0.4	2.1 ± 3.8	13.5 ± 4.9	5.4 ± 3.7	10.0 ± 4.9
`CTEQ6M`	N/A	2.8 ± 0.9	N/A	19.0 ± 10.4	N/A	20.9 ± 10.2

TABLE VI. Comparison of the shift of M_W for different PDF sets using the m_T, $p_T(\ell)$ and $p_T(\nu)$ observables, respectively. The central prediction used was `CT18NNLO` with a mass of 80,385 MeV. The uncertainties quoted are the PDF uncertainties for the given PDF set.

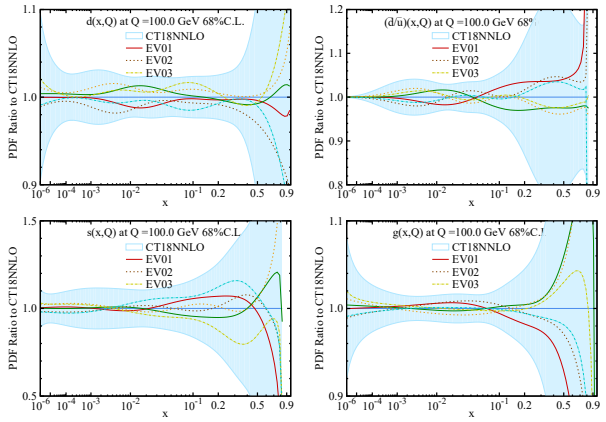

FIG. 13. Ratios of the top three pairs of eigenvector PDFs and the original CT18 NNLO error PDFs, at $Q = 100$ GeV, to the CT18 NNLO central value of d, $\bar{d}/\bar{u}$, s and g PDFs. These eigenvector PDFs were obtained after applying the ePump-optimization to the original CT18 NNLO PDFs with respect to the m_T distribution.

[1] de Blas, J. and Ciuchini, M. and Franco, E. and Goncalves, A. and Mishima, S. and Pierini, M. and Reina, L. and Silvestrini, L., (2021), arXiv:2112.07274 [hep-ph].
[2] T. Aaltonen et al. (CDF), Science **376**, 170 (2022).
[3] Y.-Z. Fan, T.-P. Tang, Y.-L. S. Tsai, and L. Wu, (2022), arXiv:2204.03693 [hep-ph].
[4] C.-T. Lu, L. Wu, Y. Wu, and B. Zhu, (2022), arXiv:2204.03796 [hep-ph].
[5] P. Athron, A. Fowlie, C.-T. Lu, L. Wu, Y. Wu, and B. Zhu, (2022), arXiv:2204.03996 [hep-ph].
[6] J. M. Yang and Y. Zhang, (2022), arXiv:2204.04202 [hep-ph].
[7] T.-P. Tang, M. Abdughani, L. Feng, Y.-L. S. Tsai, and Y.-Z. Fan, (2022), arXiv:2204.04356 [hep-ph].
[8] X. K. Du, Z. Li, F. Wang, and Y. K. Zhang, (2022), arXiv:2204.04286 [hep-ph].
[9] G. Cacciapaglia and F. Sannino, (2022), arXiv:2204.04514 [hep-ph].
[10] M. Blennow, P. Coloma, E. Fernández-Martínez, and M. González-López, (2022), arXiv:2204.04559 [hep-ph].
[11] K. Sakurai, F. Takahashi, and W. Yin, (2022), arXiv:2204.04770 [hep-ph].
[12] F. Arias-Aragón, E. Fernández-Martínez, M. González-López, and L. Merlo, (2022), arXiv:2204.04672 [hep-ph].
[13] X. Liu, S.-Y. Guo, B. Zhu, and Y. Li, (2022), arXiv:2204.04834 [hep-ph].
[14] K. S. Babu, S. Jana, and V. P. K., (2022), arXiv:2204.05303 [hep-ph].
[15] L. Di Luzio, R. Gröber, and P. Paradisi, (2022), arXiv:2204.05284 [hep-ph].
[16] J. J. Heckman, (2022), arXiv:2204.05302 [hep-ph].
[17] H. M. Lee and K. Yamashita, (2022), arXiv:2204.05024 [hep-ph].
[18] H. Bahl, J. Braathen, and G. Weiglein, (2022), arXiv:2204.05269 [hep-ph].
[19] H. Song, W. Su, and M. Zhang, (2022), arXiv:2204.05085 [hep-ph].
[20] P. Athron, M. Bach, D. H. J. Jacob, W. Kotlarski, D. Stöckinger, and A. Voigt, (2022), arXiv:2204.05285 [hep-ph].
[21] Y. Heo, D.-W. Jung, and J. S. Lee, (2022), arXiv:2204.05728 [hep-ph].
[22] A. Crivellin, M. Kirk, T. Kitahara, and F. Mescia, (2022), arXiv:2204.05962 [hep-ph].
[23] M. Endo and S. Mishima, (2022), arXiv:2204.05965 [hep-ph].
[24] X. K. Du, Z. Li, F. Wang, and Y. K. Zhang, (2022), arXiv:2204.05760 [hep-ph].

[25] K. Cheung, W.-Y. Keung, and P.-Y. Tseng, (2022), arXiv:2204.05942 [hep-ph].
[26] L. Di Luzio, M. Nardecchia, and C. Toni, (2022), arXiv:2204.05945 [hep-ph].
[27] R. Balkin, E. Madge, T. Menzo, G. Perez, Y. Soreq, and J. Zupan, (2022), arXiv:2204.05992 [hep-ph].
[28] T. Biekötter, S. Heinemeyer, and G. Weiglein, (2022), arXiv:2204.05975 [hep-ph].
[29] X.-F. Han, F. Wang, L. Wang, J. M. Yang, and Y. Zhang, (2022), arXiv:2204.06505 [hep-ph].
[30] M.-D. Zheng, F.-Z. Chen, and H.-H. Zhang, (2022), arXiv:2204.06541 [hep-ph].
[31] Y. H. Ahn, S. K. Kang, and R. Ramos, (2022), arXiv:2204.06485 [hep-ph].
[32] J. Kawamura, S. Okawa, and Y. Omura, (2022), arXiv:2204.07022 [hep-ph].
[33] A. Ghoshal, N. Okada, S. Okada, D. Raut, Q. Shafi, and A. Thapa, (2022), arXiv:2204.07138 [hep-ph].
[34] P. Fileviez Perez, H. H. Patel, and A. D. Plascencia, (2022), arXiv:2204.07144 [hep-ph].
[35] K. I. Nagao, T. Nomura, and H. Okada, (2022), arXiv:2204.07411 [hep-ph].
[36] S. Kanemura and K. Yagyu, (2022), arXiv:2204.07511 [hep-ph].
[37] K.-Y. Zhang and W.-Z. Feng, (2022), arXiv:2204.08067 [hep-ph].
[38] D. Borah, S. Mahapatra, D. Nanda, and N. Sahu, (2022), arXiv:2204.08266 [hep-ph].
[39] T. A. Chowdhury, J. Heeck, S. Saad, and A. Thapa, (2022), arXiv:2204.08390 [hep-ph].
[40] G. Arcadi and A. Djouadi, (2022), arXiv:2204.08406 [hep-ph].
[41] O. Popov and R. Srivastava, (2022), arXiv:2204.08568 [hep-ph].
[42] L. M. Carpenter, T. Murphy, and M. J. Smylie, (2022), arXiv:2204.08546 [hep-ph].
[43] K. Ghorbani and P. Ghorbani, (2022), arXiv:2204.09001 [hep-ph].
[44] A. Bhaskar, A. A. Madathil, T. Mandal, and S. Mitra, (2022), arXiv:2204.09031 [hep-ph].
[45] M. Du, Z. Liu, and P. Nath, (2022), arXiv:2204.09024 [hep-ph].
[46] D. Borah, S. Mahapatra, and N. Sahu, (2022), arXiv:2204.09671 [hep-ph].
[47] J. Cao, L. Meng, L. Shang, S. Wang, and B. Yang, (2022), arXiv:2204.09477 [hep-ph].
[48] J. Heeck, (2022), arXiv:2204.10274 [hep-ph].
[49] S. Lee, K. Cheung, J. Kim, C.-T. Lu, and J. Song, (2022), arXiv:2204.10338 [hep-ph].
[50] A. Batra, S. K. A, S. Mandal, H. Prajapati, and R. Srivastava, (2022), arXiv:2204.11945 [hep-ph].
[51] A. E. Faraggi and M. Guzzi, (2022), arXiv:2204.11974 [hep-ph].
[52] H. Abouabid, A. Arhrib, R. Benbrik, M. Krab, and M. Ouchemhou, (2022), arXiv:2204.12018 [hep-ph].
[53] V. Basiouris and G. K. Leontaris, (2022), arXiv:2205.00758 [hep-ph].
[54] J.-W. Wang, X.-J. Bi, P.-F. Yin, and Z.-H. Yu, (2022), arXiv:2205.00783 [hep-ph].
[55] R. Dcruz and A. Thapa, (2022), arXiv:2205.02217 [hep-ph].
[56] M. Aaboud et al. (ATLAS), Eur. Phys. J. C **78**, 110 (2018), [Erratum: Eur.Phys.J.C 78, 898 (2018)], arXiv:1701.07240 [hep-ex].
[57] R. Aaij et al. (LHCb), JHEP **01**, 036 (2022), arXiv:2109.01113 [hep-ex].
[58] C. Balazs and C. P. Yuan, Phys. Rev. D **56**, 5558 (1997), arXiv:hep-ph/9704258.
[59] F. Landry, R. Brock, P. M. Nadolsky, and C. P. Yuan, Phys. Rev. D **67**, 073016 (2003), arXiv:hep-ph/0212159.
[60] D. Castelvecchi and E. Gibney, Nature **604**, 225 (2022).
[61] J. Isaacson, ResBos2: Precision Resummation for the LHC Era, Ph.D. thesis, Michigan State U. (2017).
[62] T. Aaltonen et al. (CDF), Phys. Rev. D **77**, 112001 (2008), arXiv:0708.3642 [hep-ex].
[63] J. C. Collins, D. E. Soper, and G. F. Sterman, Nucl. Phys. B **250**, 199 (1985).
[64] J. Collins, Foundations of perturbative QCD, Vol. 32 (Cambridge University Press, 2013).
[65] J. C. Collins and D. E. Soper, Phys. Rev. D **16**, 2219 (1977).
[66] C. S. Lam and W.-K. Tung, Phys. Rev. D **21**, 2712 (1980).
[67] J. M. Campbell, R. K. Ellis, and W. T. Giele, Eur. Phys. J. C **75**, 246 (2015), arXiv:1503.06182 [physics.comp-ph].
[68] T.-J. Hou et al., Phys. Rev. D **103**, 014013 (2021), arXiv:1912.10053 [hep-ph].
[69] G. Bozzi, S. Catani, G. Ferrera, D. de Florian, and M. Grazzini, Nucl. Phys. B **815**, 174 (2009), arXiv:0812.2862 [hep-ph].
[70] G. Bozzi, S. Catani, G. Ferrera, D. de Florian, and M. Grazzini, Phys. Lett. B **696**, 207 (2011), arXiv:1007.2351 [hep-ph].
[71] R. D. Ball et al. (NNPDF), Eur. Phys. J. C **77**, 663 (2017), arXiv:1706.00428 [hep-ph].
[72] L. A. Harland-Lang, A. D. Martin, P. Motylinski, and R. S. Thorne, Eur. Phys. J. C **75**, 204 (2015), arXiv:1412.3989 [hep-ph].
[73] S. Alekhin, J. Bluemlein, S.-O. Moch, and R. Placakyte, PoS **DIS2016**, 016 (2016), arXiv:1609.03327 [hep-ph].
[74] A. Accardi, L. T. Brady, W. Melnitchouk, J. F. Owens, and N. Sato, Phys. Rev. D **93**, 114017 (2016), arXiv:1602.03154 [hep-ph].
[75] J. Pumplin, D. R. Stump, J. Huston, H. L. Lai, P. M. Nadolsky, and W. K. Tung, JHEP **07**, 012 (2002), arXiv:hep-ph/0201195.
[76] M. Hussein, J. Isaacson, and J. Huston, J. Phys. G **46**, 095002 (2019), arXiv:1905.00110 [hep-ph].
[77] S. Catani, D. de Florian, and M. Grazzini, Nucl. Phys. B **596**, 299 (2001), arXiv:hep-ph/0008184.
[78] W. Bizon, P. F. Monni, E. Re, L. Rottoli, and P. Torrielli, JHEP **02**, 108 (2018), arXiv:1705.09127 [hep-ph].
[79] T. Becher, M. Neubert, and D. Wilhelm, JHEP **05**, 110 (2013), arXiv:1212.2621 [hep-ph].
[80] X. Chen, T. Gehrmann, E. W. N. Glover, A. Huss, Y. Li, D. Neill, M. Schulze, I. W. Stewart, and H. X. Zhu, Phys. Lett. B **788**, 425 (2019), arXiv:1805.00736 [hep-ph].
[81] T. Becher and T. Neumann, JHEP **03**, 199 (2021), arXiv:2009.11437 [hep-ph].
[82] T. C. Rogers, Eur. Phys. J. A **52**, 153 (2016), arXiv:1509.04766 [hep-ph].
[83] R. Angeles-Martinez et al., Acta Phys. Polon. B **46**, 2501 (2015), arXiv:1507.05267 [hep-ph].
[84] J. M. Henn, G. P. Korchemsky, and B. Mistlberger, JHEP **04**, 018 (2020), arXiv:1911.10174 [hep-th].

[85] A. von Manteuffel, E. Panzer, and R. M. Schabinger, Phys. Rev. Lett. **124**, 162001 (2020), arXiv:2002.04617 [hep-ph].

[86] Y. Li and H. X. Zhu, Phys. Rev. Lett. **118**, 022004 (2017), arXiv:1604.01404 [hep-ph].

[87] S. Catani, L. Cieri, D. de Florian, G. Ferrera, and M. Grazzini, Eur. Phys. J. C **72**, 2195 (2012), arXiv:1209.0158 [hep-ph].

[88] F. Landry, R. Brock, G. Ladinsky, and C. P. Yuan, Phys. Rev. D **63**, 013004 (2001), arXiv:hep-ph/9905391.

[89] A. Bacchetta, G. Bozzi, M. Radici, M. Ritzmann, and A. Signori, Phys. Lett. B **788**, 542 (2019), arXiv:1807.02101 [hep-ph].

[90] B. U. Musch, P. Hagler, J. W. Negele, and A. Schafer, Phys. Rev. D **83**, 094507 (2011), arXiv:1011.1213 [hep-lat].

[91] B. U. Musch, P. Hagler, M. Engelhardt, J. W. Negele, and A. Schafer, Phys. Rev. D **85**, 094510 (2012), arXiv:1111.4249 [hep-lat].

[92] M. Engelhardt, P. Hägler, B. Musch, J. Negele, and A. Schäfer, Phys. Rev. D **93**, 054501 (2016), arXiv:1506.07826 [hep-lat].

[93] B. Yoon, M. Engelhardt, R. Gupta, T. Bhattacharya, J. R. Green, B. U. Musch, J. W. Negele, A. V. Pochinsky, A. Schäfer, and S. N. Syritsyn, Phys. Rev. D **96**, 094508 (2017), arXiv:1706.03406 [hep-lat].

[94] P. Shanahan, M. L. Wagman, and Y. Zhao, Phys. Rev. D **101**, 074505 (2020), arXiv:1911.00800 [hep-lat].

[95] P. Shanahan, M. Wagman, and Y. Zhao, Phys. Rev. D **102**, 014511 (2020), arXiv:2003.06063 [hep-lat].

[96] Q.-A. Zhang et al. (Lattice Parton), Phys. Rev. Lett. **125**, 192001 (2020), arXiv:2005.14572 [hep-lat].

[97] M. Schlemmer, A. Vladimirov, C. Zimmermann, M. Engelhardt, and A. Schäfer, JHEP **08**, 004 (2021), arXiv:2103.16991 [hep-lat].

[98] Y. Li et al., Phys. Rev. Lett. **128**, 062002 (2022), arXiv:2106.13027 [hep-lat].

[99] P. Shanahan, M. Wagman, and Y. Zhao, Phys. Rev. D **104**, 114502 (2021), arXiv:2107.11930 [hep-lat].

[100] M.-H. Chu et al. (LPC), (2022), arXiv:2204.00200 [hep-lat].

[101] P. A. Zyla et al. (Particle Data Group), PTEP **2020**, 083C01 (2020).

[102] C. Schmidt, J. Pumplin, C. P. Yuan, and P. Yuan, Phys. Rev. D **98**, 094005 (2018), arXiv:1806.07950 [hep-ph].

[103] T.-J. Hou, Z. Yu, S. Dulat, C. Schmidt, and C. P. Yuan, Phys. Rev. D **100**, 114024 (2019), arXiv:1907.12177 [hep-ph].

[104] J. Pumplin, Phys. Rev. D **80**, 034002 (2009), arXiv:0904.2425 [hep-ph].